Detrimental Effects of Capacitance on High-Resistance-Grounded Mine Distribution Systems

Joseph Sottile, *Senior Member, IEEE*, Steve J. Gnapragasam, Thomas Novak, *Fellow, IEEE*, and Jeffrey L. Kohler, *Senior Member, IEEE*

***Abstract*—Modern underground coal mines can be very large, having a total connected load in excess of 15 000 hp. These mines generally have many miles of high-power conveyor belts and 15 or more miles of high-voltage power cables at distribution voltages of 12.47, 13.2, 13.8, or 14.4 kV. The shielded cables used in mine power distribution systems have a significant level of capacitance, on the order of 110 pF/ft. This level of capacitance, in an extensive power distribution system at today's voltage levels, can cause significant charging currents during a ground fault. This paper addresses the potential detrimental effects of capacitance charging currents during line-to-ground faults in mine power distribution systems. A representative mine power system is modeled, and simulations with faults at various locations are conducted to evaluate the effects of this capacitance on the level of fault current and relay selectivity. This paper also includes results of capacitance measurements made on mine power feeder cables used to validate the simulation model.**

***Index Terms*—Charging current, ground fault.**

I. Introduction

The PRIMARY goals of a power-system protection scheme are to prevent personnel injury, minimize damage to the power system, and minimize the extent and duration of the adverse condition during various types of faults. With respect to ground faults, the protection system should limit the fault current and energy, quickly and reliably detect the fault, and deenergize only the offending section of the power system (selectivity).

A high-resistance grounded system is defined as a system, in which $R_0 \leq X_c$, where R_0 is the per-phase zero-sequence resistance of the system and X_c is the distributed per-phase system-to-ground capacitive reactance [1]. In practical mine power systems, the zero-sequence resistance is dominated by the neutral grounding resistor (NGR), so a high-resistance grounded system requires that $R_N \leq 1/3X_c$, where R_N is the value of the NGR.

Ungrounded systems have no intentional connection to ground. They are, of course, grounded by the distributed capacitance of phase windings and power-system conductors. Ungrounded systems have the disadvantage of subjecting the system to severe overvoltages during certain types of ground faults by repetitive charging of the system capacitance or by resonance between the system capacitance and equipment and system inductance. Systems in which the value of the NGR exceeds the limit for high-resistance grounding begin to exhibit the disadvantageous characteristics of an ungrounded system [2].

It is a common practice in modern mine power systems to size the NGR to limit the neutral current to 25 A and to use a pickup setting of 40% of this current limit, i.e., 10 A. This is done to comply with Part 75.801 of Title 30 of the Code of Federal Regulations, which requires that the NGR be of proper ohmic value to limit the voltage drop in the grounding circuit external to the resistor to not more than 100 V during fault conditions [3]. Because modern mine power systems can be very extensive, with 15 or more miles of shielded high-voltage distribution cable, the distributed capacitance of these power systems combined with the low limit on neutral ground current can create situations in which the definition of a high-resistance grounded system is violated and the system begins to exhibit the characteristics of an ungrounded system.

This paper examines the modern grounding practice commonly employed in underground coal mines and studies the potential for adverse effects caused by distributed system capacitance. The analysis conducted involves the use of a Spice software to model an underground coal mine distribution system. Ground faults are simulated at various points and the effects of distributed system capacitance on fault current levels, relay selectivity, and overvoltages are examined.

II. Power-System Simulation Model

A. Power-System Overview

The mine power system that has been simulated is a 12.47-kV expanded radial distribution system supplying two

J. Sottile is with the University of Kentucky, Lexington, KY 40506-0107 USA (e-mail: jsottile@ieee.org).

S. J. Gnapragasam was with the University of Kentucky, Lexington, KY 40505-0107 USA. He is now with ADS Consulting Engineers, New York, NY 10001 USA (e-mail: Steve.Gnapragasam@adsce.com).

T. Novak is with Virginia Polytechnic Institute and State University, Blacksburg, VA 24061 USA (e-mail: tomnovak@vt.edu).

J. L. Kohler is with the National Institute for Occupational Safety and Health, Pittsburgh, PA 15236 USA (e-mail: jtk4@cdc.gov; JKohler@cdc.gov).

Color versions of Figs. 2, 4, and 5 are available at http://ieeexplore.ieee.org.

Digital Object Identifier 10.1109/TIA.2006.880844

TABLE I
SUMMARY OF MAJOR ELECTRICAL LOADS

Load	Number	Unit Power (hp)	Total Power (hp)
CM Section	2	1350	2700
Longwall Section	1	5100	5100
Belt Drive	4	725	2900
Belt Drive	3	1000	3000
Belt Drive	1	1400	1400
Motor Pit	1	400	400
Total	-----	-----	15,500

TABLE II
SUMMARY OF DISTRIBUTION SYSTEM

Utility SCC	126.9 MVA
Utility X/R Ratio	14.41
Borehole Cable	850 ft, 500 kcmil, 15 kV, MP-GC
Distribution Cables	75,200 ft (total) 4/0, 15 kV, MP-GC
Pf Correction	3000 kvar at Substation
Transformers	Z = 5%, X/R = 4

continuous-miner (CM) sections and one longwall (LW) face. The borehole cable is 500-kcmil MP-GC, and the remainder of the distribution system consists of 4/0 MP-GC. Typical loading requirements for conveyor belt drive motors, LW, and CM equipment were used to develop the model. Tables I and II summarize the relevant information about the distribution system and Fig. 1 shows a one-line diagram of the power system. Note that only major loads have been included in the system model.

B. Model Development

Because interest was focused on studying the effects of distribution-system ground faults, several simplifications were made in developing the system model for simulation in B^2Spice.

The utility supply is modeled as a three-phase wye-connected voltage source in series with resistance and inductance values determined from the nominal system voltage, short circuit capacity, and X/R ratio (listed in Table II).

Load modeling was simplified by combining the power requirements of the individual loads at each production section into one equivalent load (as listed in Table I). The resulting loads were modeled as three wye-connected resistance and inductance values determined from the total rated power, nominal system voltage, and assumed values for power factor (0.90 lagging), efficiency (90%), and load factor (0.85). Although this method of modeling (i.e., modeling motor loads as constant impedance values instead of constant power values) would not be preferred for detailed load flow analysis, it is adequate for modeling ground faults in high-resistance grounded systems.

Rather than modeling the conveyor belt and production section transformers as coupled coils, they were modeled as series resistance and inductance elements connected between the cables and the loads. The resistance and inductance values were determined by converting the transformer per unit impedances to the 12.47-kV distribution voltage. Fig. 2 shows the portion of the simulation model for a 1500-kVA transformer supplying a 1350-hp CM section. Table III summarizes the transformer data for each size of transformer. Note that, while there are only three different sizes of transformers listed in this table, there are 12 transformers in the system.

Mine distribution cables are represented as lumped parameter elements connected in a nominal-π configuration. Several sources were consulted for resistance and 60-Hz reactance values for 500 kcmil and 4/0 mine power feeder, and it was determined that the values differed very slightly, if at all. Therefore, typical 90 °C resistance values (per 1000 ft) of 0.027 and 0.063 Ω, and 60-Hz reactance values of 0.031 and 0.035 Ω for 500 kcmil and 4/0, respectively, for 15-kV MP-GC cables were used [4].

Although general approximations can be used to estimate the cable capacitance, it was decided that the capacitance values used in the simulation model should be based on a representative cable used commonly in underground coal mine distribution systems. By doing this, comparisons could be made with capacitance measurements on the same type of cable. The brand and type of cable selected for this paper is an AmerCable Tiger Brand TB2-604, Type MP-GC, 3/C, 15-kV cable. This cable was chosen because it is widely used in distribution systems, and the dimensions required for calculating capacitance were available.

The per-phase capacitance from line to ground can be calculated from the following relationship [4]:

$$C = \frac{7.354\varepsilon}{\log_{10}\left(1+\frac{2t}{d}\right)}\left[\frac{\text{pF}}{\text{ft}}\right] \tag{1}$$

where

- ε dielectric constant of the insulation;
- t thickness of the conductor insulation;
- d diameter under the insulation.

For ethylene propylene rubber (EPR) insulation at this voltage class, the typical SIC value is 3.2, and the maximum value is 4.0. The typical value of 3.2 was used because it is what would be expected in the field, although using a value of 4.0 would be more conservative because it would predict the maximum expected capacitance. The strand diameter, extruded strand shield, and insulation thickness values used for calculating capacitance of this cable are listed in Table IV [5].

The extruded strand shield is a semiconductor surrounding the power conductor and is added to provide a uniform radial voltage stress distribution by filling interstices along the perimeter of the power conductor. When the strand shield is added, the conductor is placed in tension, and the conductor diameter is reduced by approximately two mils below the nominal value. As a result, the diameter under the insulation for a 4/0 cable is

$$d = (0.510) + (2 \times 0.018) = 0.546 \text{ in.} \tag{2}$$

As an example, the resulting per-phase capacitance per foot for a 4/0 cable is

$$C = \frac{7.354\varepsilon}{\log_{10}\left(1+\frac{2t}{d}\right)} = \frac{7.354 \times 3.2}{\log_{10}\left(1+\frac{2\times 0.175}{0.546}\right)} = 109.4\ \frac{\text{pF}}{\text{ft}}. \tag{3}$$

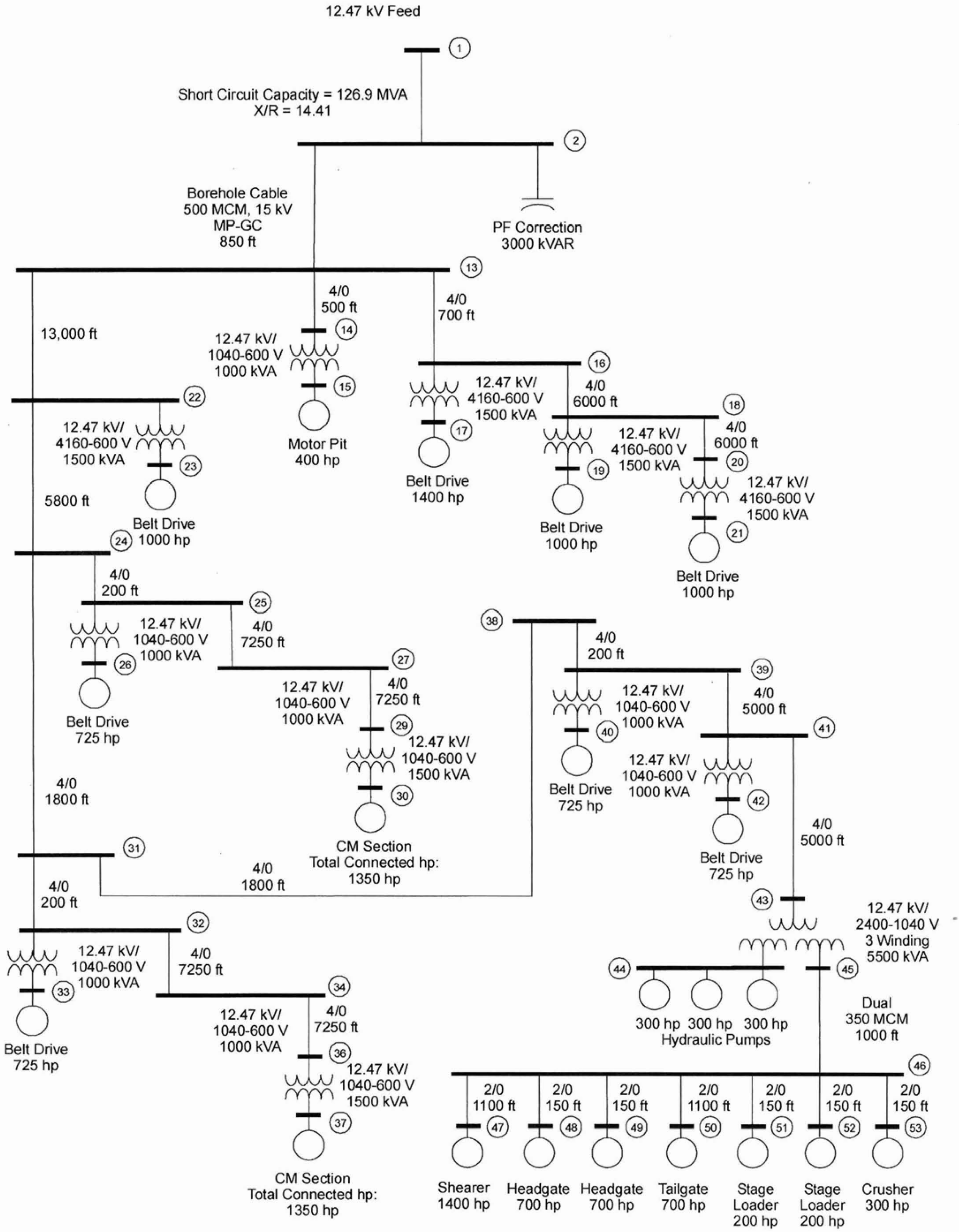

Fig. 1. One-line diagram of mine distribution system.

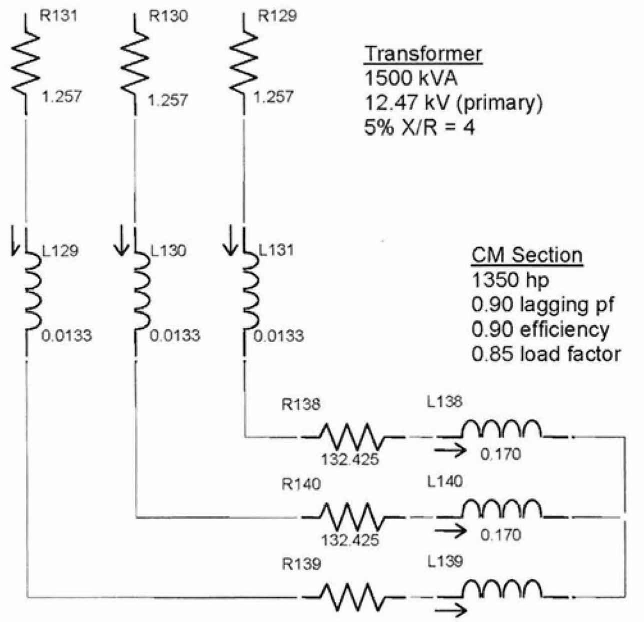

Fig. 2. Portion of simulation model representing 1500-kVA transformer supplying a 1350-hp CM section.

TABLE III
TRANSFORMER SUMMARY

Voltage (V)	kVA	Z_{pu}	X/R	R (Ω)	L (H)
12,470	1,000	0.05	4	1.885	0.0200
12,470	1,500	0.05	4	1.257	0.0133
12,470	5,500	0.05	4	0.343	0.00364

TABLE IV
CABLE PARAMETERS FOR CALCULATING CAPACITANCE

Cable type:	MP-GC 3/C 15kV (TB2-604™)
Conductor size:	4/0
Strand diameter:	0.512 in
Extruded strand shield:	0.018 in thick (typical)
Insulation thickness:	0.175 in (EPR)

TABLE V
RESISTANCE, INDUCTANCE, AND CAPACITANCE VALUES FOR MINE DISTRIBUTION CABLES

Conductor Size	Resistance (Ω/1000 ft)	Inductance (mH/1000 ft)	Per-Phase Capacitance (μF/1000 ft)
500 kcmil	0.027	0.0821	0.1520
4/0 awg	0.063	0.0928	0.1094

Table V provides a summary of the resistance, inductance, and capacitance values used for the 500-kcmil borehole cable and 4/0 distribution cables used in the mine simulation model.

III. MODEL VERIFICATION

A. Cable Capacitance Verification

Although the capacitance calculations are relatively straightforward, the authors believe that, considering the nature of this paper, it is important to provide verification by comparing calculations with measurements. Therefore, an experiment was conducted, in which the capacitance of a piece of mine power feeder was measured. The selected cable was a 500-ft section of 15-kV 4/0 MP-GC mine power feeder manufactured by AmerCable, which is the same size and type used in the capacitance calculations.

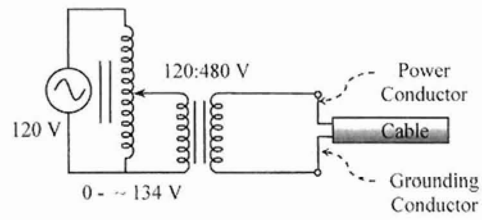

Fig. 3. Experimental setup for measuring capacitance.

The experimental procedure consisted of energizing the open-circuited cable from line to ground and measuring the voltage and current. These values were then used to compute the 60-Hz reactance, from which the capacitance could be determined. The cable was also hi-pot tested prior to making the measurements to ensure it had no insulation defects that would cause abnormally high leakage current.

Power for the tests was obtained from a standard 120-V outlet and fed into a 120-V variac that was connected to a 120 : 480 V step-up transformer. Although the variac was specified as 120 V, the actual output range was approximately 0–134 V. This provided a variable ac voltage range of approximately 0–536 V for the tests. Five feet of insulated #12 awg conductor was used as lead wire to connect the transformer to the cable power and grounding conductors. Fig. 3 illustrates the experimental setup.

Measurements were acquired by connecting a Tektronix P6009 low-input-capacitance, high-voltage probe between line and ground and clamping an AEMC Model K110 DC/AC MicroProbe current probe around the #12 awg lead wire. Signals were acquired by a Fluke 123 ScopeMeter. During the experiments, some harmonic distortion of the current waveform was observed. Although this distortion was not large compared to the 60-Hz signal, it caused difficulties in accurately determining the phase shift between voltage and current. Notwithstanding, observations indicated that the current led the voltage by approximately 80°. Because this phase shift was difficult to determine accurately, and the reactive component of current leading voltage by approximately 80° is nearly equal to a purely reactive current, no attempt was made to separate the real and reactive components, and the total measured current was used to determine capacitance.

Voltage and current measurements were based on the true rms value indicated by the Fluke ScopeMeter. These values were also verified by connecting the probes to a Fluke Model 87 Multimeter. In addition, because the Fluke 87 Multimeter has a capacitance meter, it was used to measure capacitance to provide additional verification. The insulation was discharged before connecting the capacitance meter to the cable to eliminate the possibility of having a residual charge on the insulation. Table VI provides a summary of the capacitance measurements made on the 15-kV cable.

Comparison of these measurements with calculated values given in (3) shows very good agreement. The capacitance calculation for 500 ft of 15-kV 4/0 MP-GC is $0.1094/2 = 0.0547\ \mu$F per phase. From Table VI, the average measured value is

TABLE VI
RESULTS OF TESTS ON 15-kV 4/0 MINE POWER FEEDER

Measurement	Voltage (V, rms)	Current (A, rms)	Capacitance (μF)
1	300 V	5.68 mA	0.0502 μF
2	530 V	9.87 mA	0.0494 μF
3*	NA	NA	0.0506 μF

* Measurement 3 is the result of a Fluke 87 Multimeter used in capacitance mode.

TABLE VII
FAULT AND NEUTRAL GROUNDING RESISTOR CURRENTS FOR VARIOUS GROUND FAULTS

Faulted Cable	NGR Current (A, rms)	Fault Current (A, rms)	Prefault Line Voltage (V, rms)
2-13	24.6	71.9	12,405
13-16	24.6	71.7	12,181
18-20	24.5	71.4	12,120
31-32	22.7	65.8	11,289
34-36	22.6	65.6	11,249
41-43	22.4	64.9	11,124

0.050 μF, which is a difference of less than 10% from the calculated value.

B. Simulation Verification

Because the model is relatively extensive (over 300 nodes, over 140 resistors, over 140 inductors, and over 100 capacitors), it was important to verify it before simulating ground faults. This was accomplished by running the simulation and using peak values and zero-crossing times to determine individual phasor values. Phasors were computed for the loads, and in each case, the voltages and currents were balanced, and the power factor was 0.90 lagging. Because the loads were necessarily modeled as constant impedance elements instead of constant power loads, the total system power was less than the specified power requirements due to voltage drops in the branches. However, for the purposes of this paper, this difference was inconsequential.

IV. RESULTS OF ANALYSES

A series of ground-fault simulations were conducted to determine the effect of distributed capacitance on the level of fault current and relay selectivity in high-resistance grounded distribution systems. In all simulations, an NGR current limit of 25 A was used because this value is a common limit currently used in coal mines to comply with regulations. The pickup was assumed to be 40% of the NGR current limit.

The first set of simulations consisted of observing the level of fault current and NGR current for ground faults at various points in the distribution system. The fault locations included the service point, the bottom of the borehole, the distribution cable to one of the CM sections, the distribution cable to the LW, and the distribution cable to two main belt drives. Table VII lists the faulted branches, the current through the NGR, the fault current, and the prefault line voltage. Results indicate that the fault current exceeds the NGR current by a factor of nearly three in all cases. The table also shows that the fault and NGR current decrease slightly with distance from the source due to reduction of the fault voltage with distance from the source.

Because the level of fault current significantly exceeds the NGR limit, simulations were conducted to determine the impact on relay selectivity during a ground fault in the distribution system. The first case presented is a line-to-ground fault in the cable connecting bus 13 to bus 16. There is a triple-breaker switchhouse at bus 13 (i.e., bottom of the borehole) and all three outgoing circuits are protected by a relay and circuit breaker.

A summary of the zero-sequence currents ($3I_{A0}$) for each of the branch circuits is given in Fig. 4. (The fault and NGR currents were given in Table VII.) This figure illustrates that the maximum zero-sequence current is in the faulted branch, and that very little zero-sequence current flows in the short circuit to the motor pit. However, the zero-sequence current in the branch circuit feeding the CM sections and LW exceeds the ground-fault pickup setting by a factor of five. Therefore, in this situation, selectivity is lost, and it is likely that the circuit breaker in this branch would trip when a ground fault occurs in the branch between bus 13 and 16.

Fig. 5 shows another situation, in which the line-to-ground fault was located in branch 31–32, and the zero-sequence current in branch 31–38 (feeding the LW) was computed. In this case, the charging current is essentially equal to the pickup value of 10 A; therefore, this is another situation where selectivity would be lost.

It is a relatively straightforward process for mine operators to evaluate their particular system for situations where loss of relay selectivity is likely to occur. The process involves estimating the cable capacitance for the portion of the system in question and using that capacitance to estimate the charging current. To illustrate, consider the situation in which the fault is in branch 13–16, and the zero-sequence current in branch 13–22 is to be predicted. The per-phase capacitance for the distribution cable is approximately 110 pF/ft, and there are 62 000 ft of cable in the distribution system for the remainder of the mine supplied through branch 13–22. The total per-phase capacitance is therefore 6.82 μF, which is a 60-Hz reactance of $-389\ \Omega$ per phase. The three-phase zero-sequence current flowing in this branch can be estimated by dividing the line-to-neutral voltage by one-third of the per-phase reactance

$$|3I_{A0}| \approx \frac{12\,181}{\sqrt{3} \times 129.6} = 54.3 \text{ A}. \tag{4}$$

This value compares very well with the simulation result of 54.6 A. Repeating this calculation for the zero-sequence current in branch 31–38 for a ground fault in branch 31–32 yields an estimate of 9.7 A compared with the simulation result of 9.8 A.

Note that in these examples the prefault voltage was used so that an accurate comparison with the simulation results could be made. However, in practical situations the nominal system voltage would be used.

Another aspect of a power system in which the charging current exceeds the NGR current is the rise in voltage for a resonant fault condition. To examine this, a fault with an inductive reactance equal to the capacitive reactance of the system

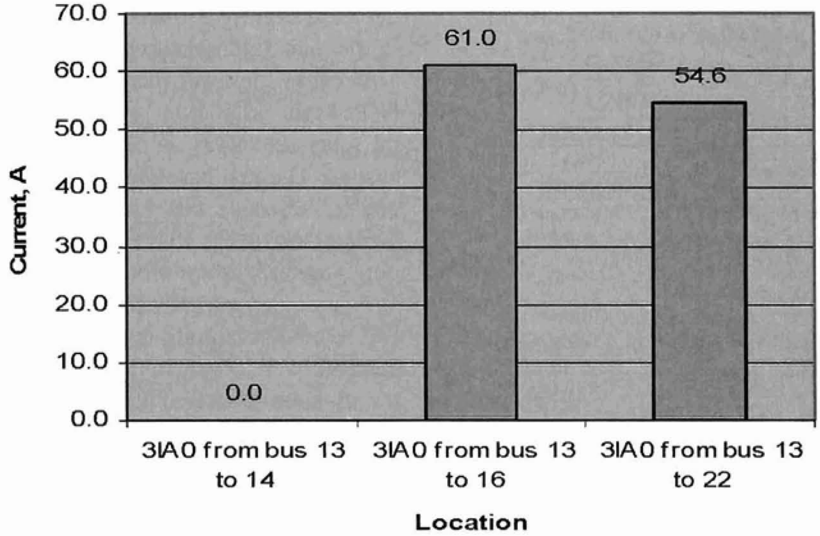

Fig. 4. Zero-sequence current for a line-to-ground fault in branch connecting bus 13 to bus 16.

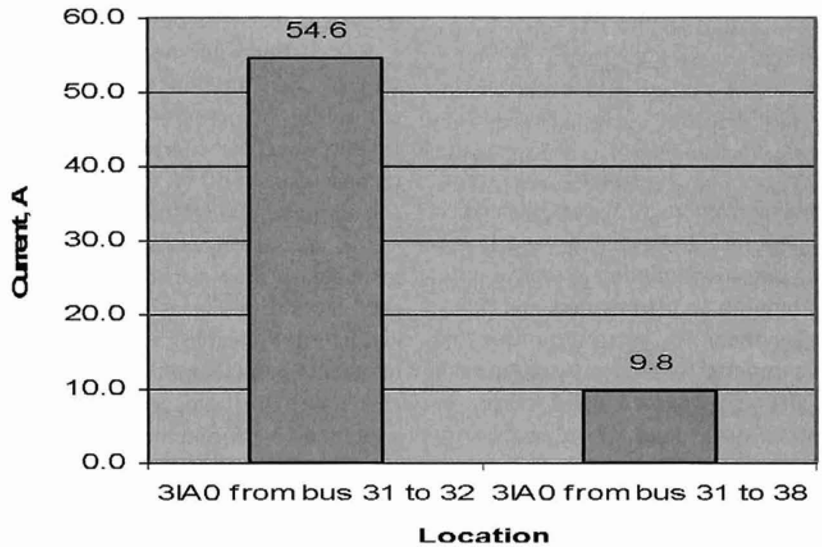

Fig. 5. Zero-sequence current for a line-to-ground fault in branch connecting bus 31 to bus 32.

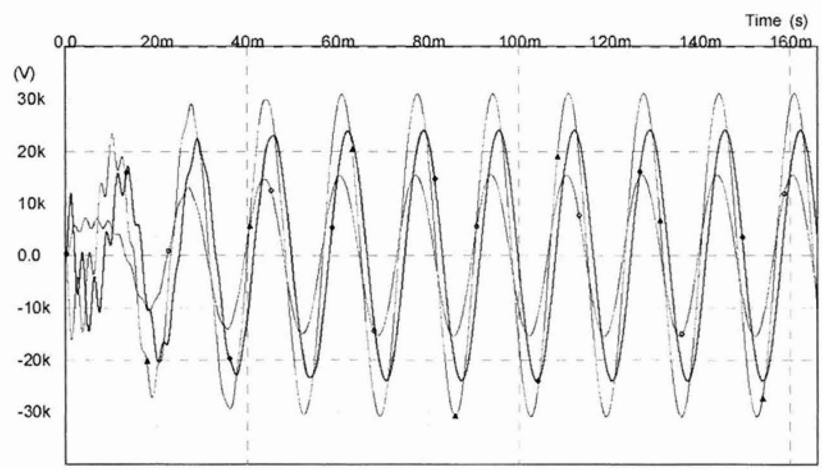

Fig. 6. Line-to-ground voltages for a resonant fault condition.

(not including the power factor correction capacitors) was introduced at bus 36, and the simulation was run for approximately ten cycles. The result, shown in Fig. 6 for a fault through a 281-mH inductance, indicates that the system would be subjected to a rise in voltage of approximately three times the rated voltage for a resonant fault condition.

V. Conclusion

Modern mine power systems can have a significant amount of distributed system capacitance. In certain cases, this capacitance and the practice of limiting the NGR current to 25 A can create situations that violate the definition of a high-resistance grounded system. For example, in the power system presented in this paper, which is based on an actual mine distribution system, the per-phase distributed capacitance is 8.36 μF, which has a 60-Hz reactance of $-317.4\ \Omega$. Therefore, the value of the NGR should be less than 106 Ω for this system to comply with the definition of high-resistance grounding. However, in practice, the resistor would be approximately 288 Ω in order to limit the NGR current to 25 A. Simulations have demonstrated that the fault current is nearly three times the NGR current limit, the system is prone to loss of selectivity, and is also susceptible to damage from overvoltages for a resonant fault condition.

References

[1] *IEEE Recommended Practice for Grounding of Industrial and Commercial Power Systems*, IEEE Std. 142-1991, 1996.

[2] *IEEE Recommended Practice for Protection and Coordination of Industrial and Commercial Power Systems*, IEEE Std. 242-2001, 2001.

[3] 30 CFR 75.801, "Title 30 of the Code of Federal Regulations," *Mineral Resources*, Office Federal Register National Archives Records Administration, 2003.

[4] *Mining Cable Engineering Handbook*, The Anaconda Company, Anaconda, MT, 1977.

[5] M. Fuller, private communication, *AmerCable*, Mar. 2004.